

Capillary forces on millimeter-scale sediment particles: Experimental measurements and theoretical estimations

Nirmalya Chatterjee¹, Sergey Lapin² and Markus Flury¹

¹Dept. of Crop and Soil Sciences, Puyallup, Washington State University; ²Dept. of Mathematics, Pullman, Washington State University

Goal and Objective

The **overall objective** of this project is to understand the mechanism of transport of contaminants, both direct transport and facilitated transport by colloids, in the vadose zone.

The **specific objective** is to measure the capillary forces on mm-scale particles due to moving air-water interfaces. The particles were obtained from the vadose zone under the waste tanks at the Hanford Site in Washington State. We then compare the experimentally measured forces with those obtained using theoretical calculations.

We **hypothesize** that:

- Capillary forces are best approximated by assuming particles to be ellipsoidal in shape, rather than a spherical shape
- Surface roughness and irregularity of natural sediment particle shapes enhance capillary forces by considerable amounts leading to increased mobilization of particles
- Calculations on mm-scale particles can be extrapolated to colloidal scale particles which have been implicated in facilitated contaminant transport.

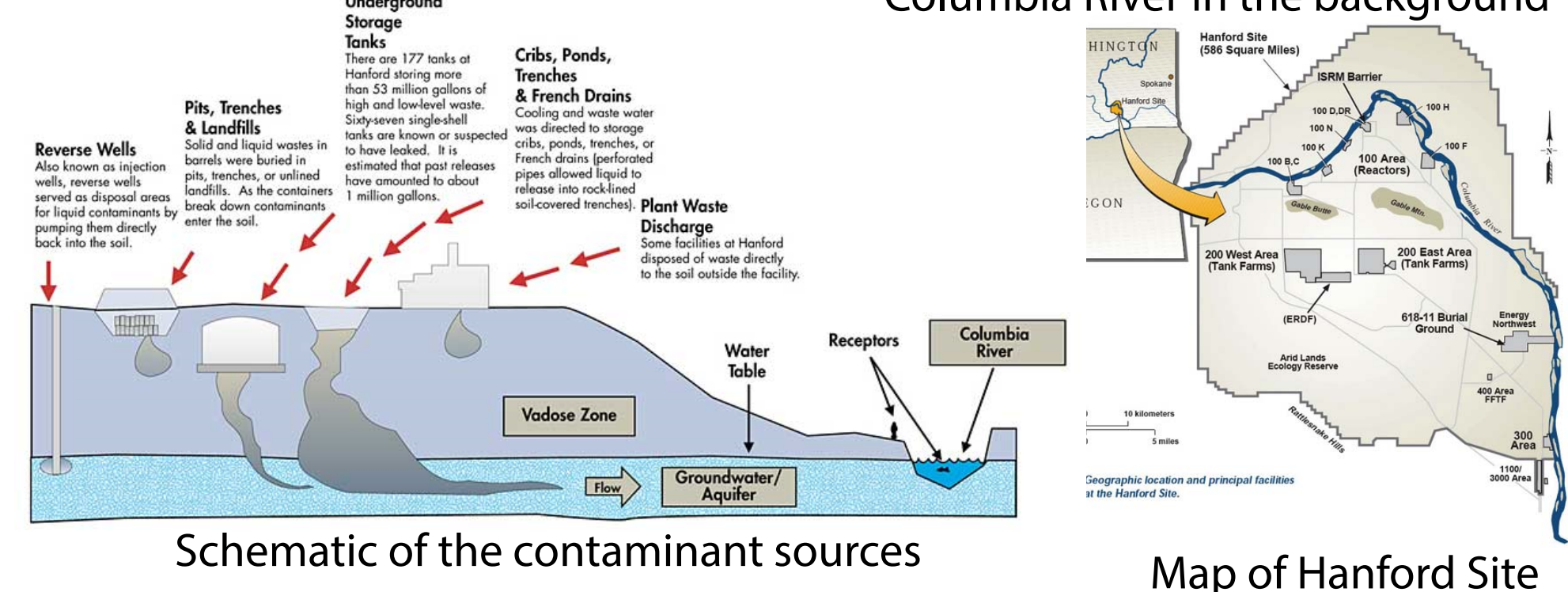
Background

- The Hanford Nuclear Site was established in 1943 as a Plutonium production facility for the US nuclear weapons production.
- Millions of gallons of low-level radioactive and hazardous waste (caustic solutions from dissolved fuel rods, sludge and solid wastes) have been dumped into the ground.
- Mobility of radioactive wastes in the semi-arid soils of the Hanford geological formation is expected to be limited because of slow vertical water movement in the soils.
- Laboratory studies using Hanford sediments indicated colloid-facilitated radioactive contaminant transport in the soils as a major cause of contaminant mobilization – in both saturated and unsaturated soil conditions. Such potential transport events may occur during strong infiltration conditions like localized thunderstorms and Chinook wind (warm and humid coastal winds from the Pacific Ocean) induced rapid snow-melts.
- Capillary forces and DLVO forces (electrostatic and van der Waals) are the most important forces acting on colloidal size particles during mobilization.

Hanford Site



Hanford tanks under construction, 1940s Aerial view of the Hanford Site with the Columbia River in the background



Schematic of the contaminant sources

Map of Hanford Site

Theory



For axisymmetric particles, the capillary rise z_c , the horizontal distance of the three-phase contact line from the z-axis, x_c , and the angle of inclination of the curved interface from the undisturbed interface, ϕ_c , is:

$$z_c = \frac{k_0(x_c)}{k_1(x_c)} \sin \phi_c$$

where the functions $k_0(x)$ and $k_1(x)$ are the modified Bessel functions of the second kind of orders 0 and 1 respectively.

- The force balance (net force \mathbf{f}) on an axisymmetric particle is:

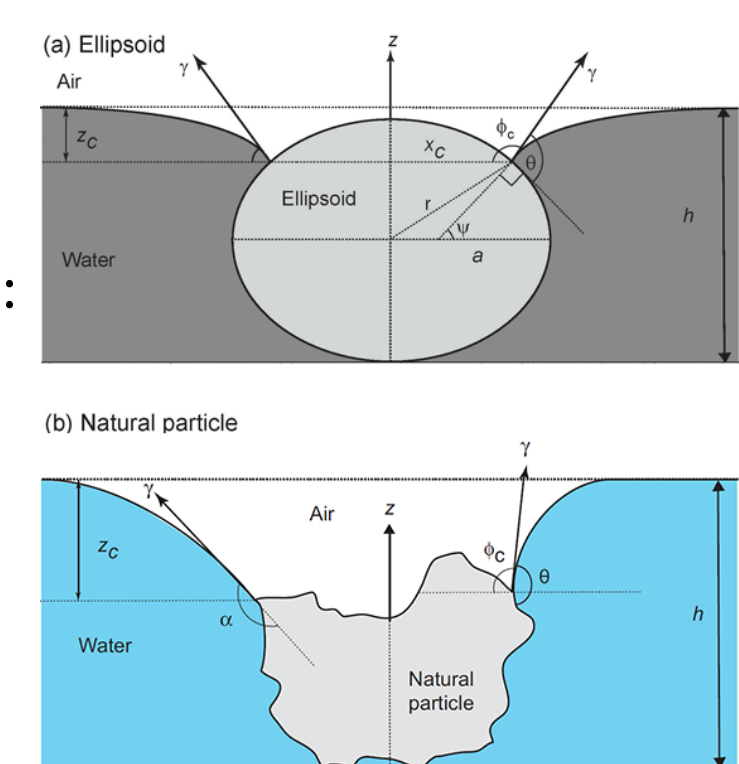
$$\mathbf{f} = \mathbf{f}_s + \mathbf{f}_b + \mathbf{f}_p$$

where \mathbf{f}_s is the surface tension force, \mathbf{f}_b is the buoyancy force, and the \mathbf{f}_p is the hydrostatic pressure force.

- The pinning can be described by the Gibbs extension of the Young Equation:

$$\theta_0 < \theta < 180^\circ - \alpha + \theta$$

where θ_0 is the equilibrium contact angle, θ is the actual contact angle, and, α is the wedge angle at the pinned contact line

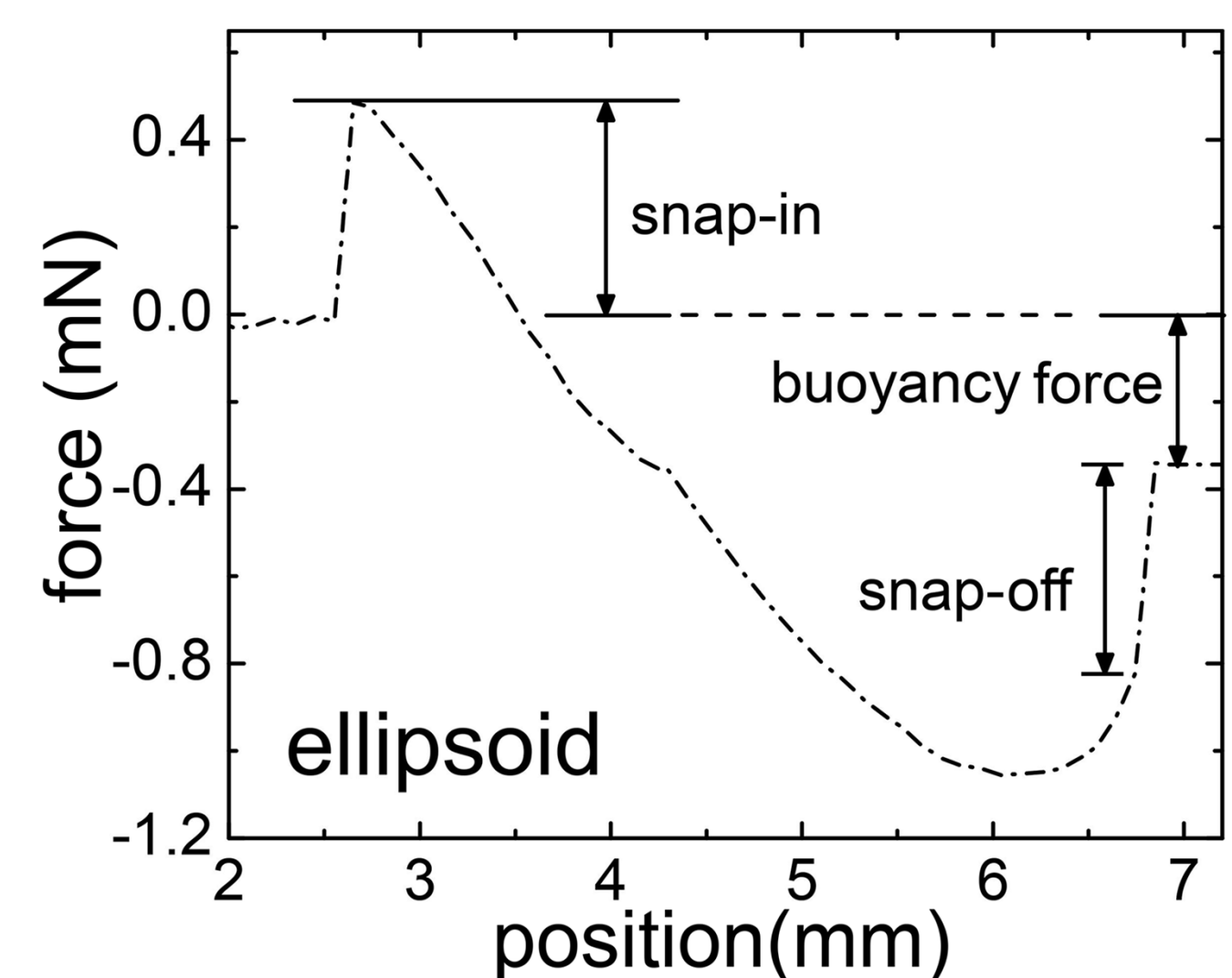


Floating coins and a water strider showing the effect and importance of capillary forces. The capillary forces are strong enough to counter gravitational forces.

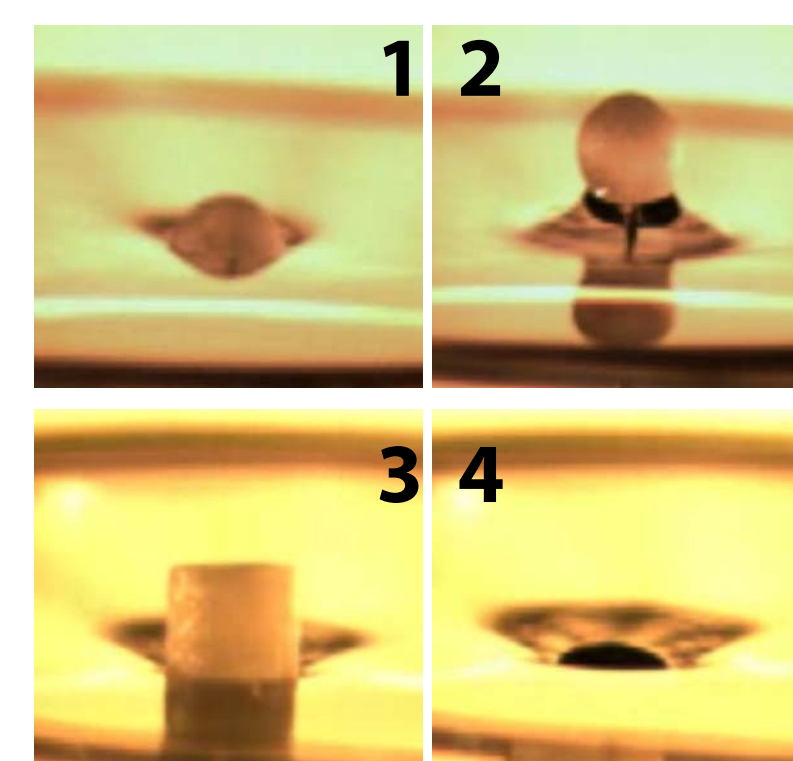
Experimental Methods



Tensiometer with microbalance, beaker and a Wilhelmy plate. Inset: a sediment particle mounted on a J-hook

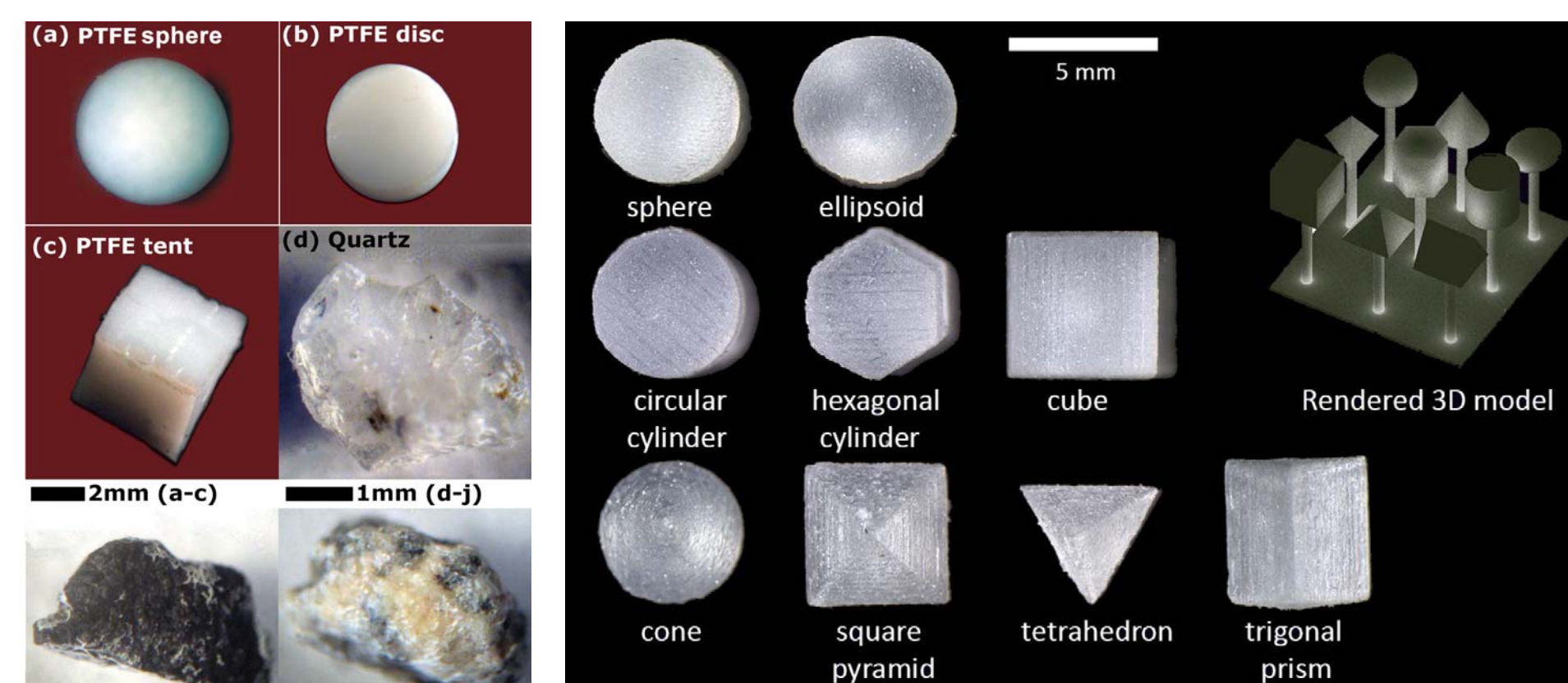


Schematic of a force-position curve obtained during immersion of a sediment particle. **x-axis** is the uncorrected position of the particle vis-à-vis the air-water interface, **y-axis** is the capillary force on the particle due to the air-water interface as measured on the microbalance.



Frames from 1000fps movies of 3D printed poly-acrylate particles showing different phenomena: (a) advancing (1-immersion) and receding (2-emersion) contact angles with a sphere (b) bottom (3) and top (4) edge pinning of air-water interface with a circular cylinder.

Experimental Results

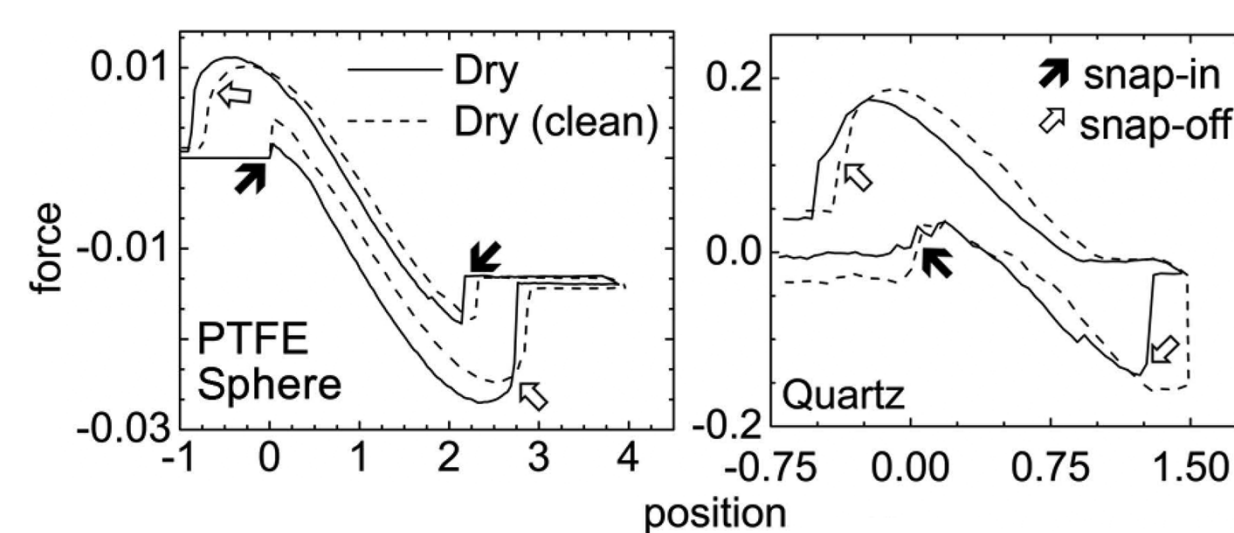


Dissection scope view of model polyacrylate 3D printed particles

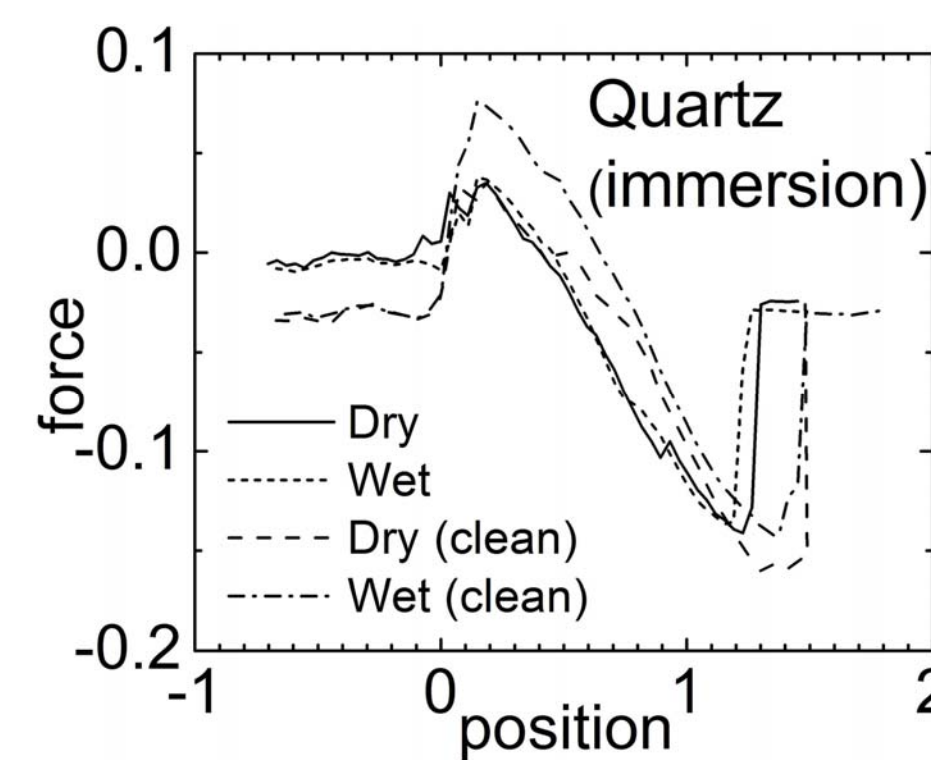
Particle	Volume equivalent radius (mm)	Max. (negative) capillary force (mN)
PTFE sphere	3.17	-1305
PTFE disk	2.09	-1292
PTFE tent	2.25	-1204
Basalt	1.15	-537
Granite	1.17	-467
Hematite	1.00	-279
Magnetite	0.79	-422
Mica	0.85	-526
Milky Quartz	1.07	-7
Quartz	1.13	-402

Set of immersion curves of a quartz sediment particle before and after solvent cleaning.

Table 1: Particle radii and maximum capillary forces on them due to a moving air-water interface



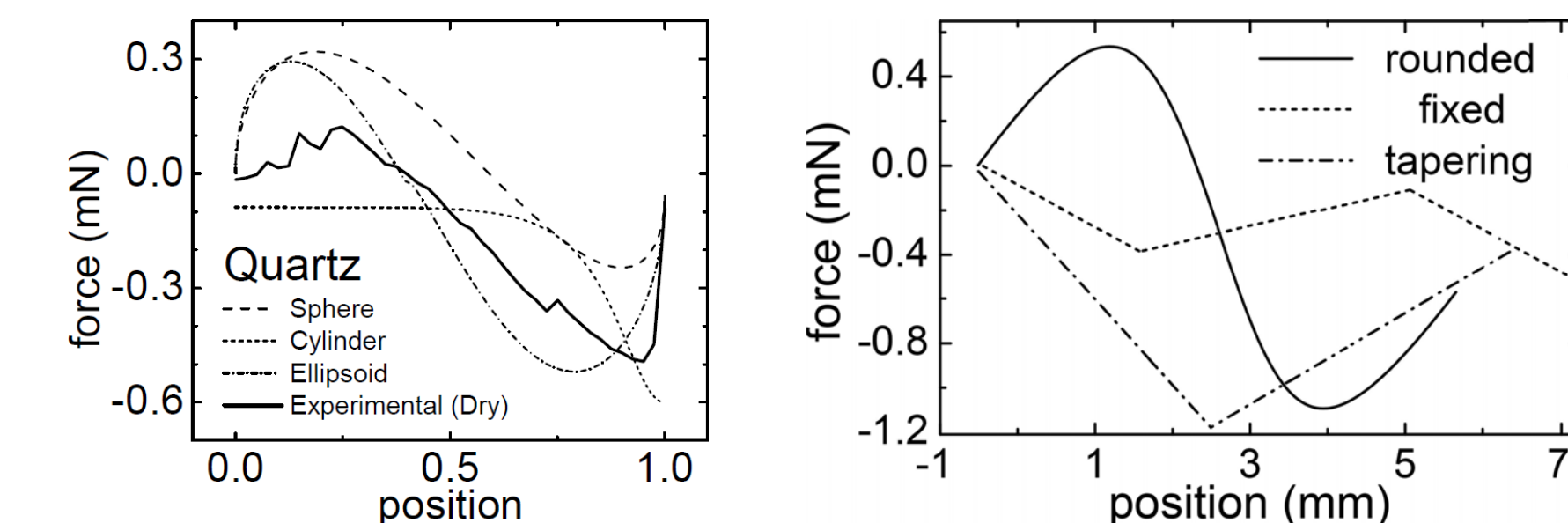
Immersion and emersion (1 cycle) force-position curve of a model PTFE sphere and a quartz sediment particle in dry condition, before and after cleaning with organic solvents.



Theoretical Results

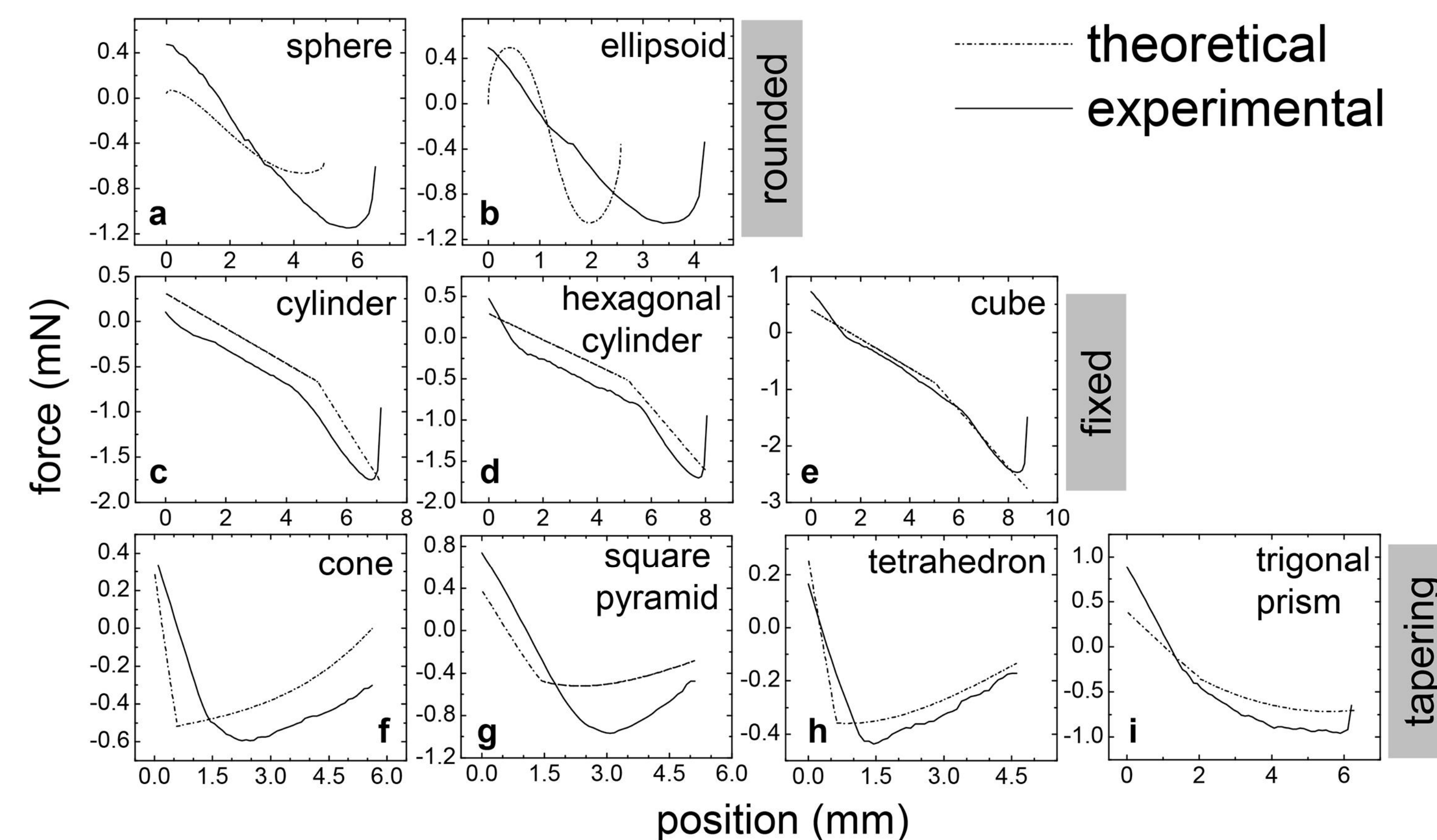
Particle	Experimental capillary force (max) (mN)	Theoretical forces (mN)	
		Spherical	Ellipsoidal
PTFE sphere	-1305	-2150	--
PTFE disk	-1292	-1510 (cylinder)	--
PTFE tent	-1204	-1096	-1446
Basalt	-537	-221	-738
Granite	-467	-297	-479
Hematite	-279	-284	-420
Magnetite	-422	-180	-377
Mica	-526	-116	-559
Milky Quartz	-7	-396	-479
Quartz	-402	-247	-472

Table 2: Comparison of maximum capillary forces (Experimental and Theoretical)



Comparison of experimental and theoretically calculated immersion curves assuming a spherical, ellipsoidal and cylindrical shape. Normalized dimensions of a **quartz** particle

Schematic of expected force-position curves of particles of three different categories of cross-sections.



Comparison of the experimental and theoretically reconstructed force-position curves for 9 different model particles of fixed shapes. The particles are classified into three different categories based on the variation of their cross-sections along their z-axes. Particles with fixed and tapering cross-sections, show a pronounced pinning of the moving air-water interface at the top and bottom edges, respectively – which were taken into consideration by calculating the force-position curve with non-equilibrium contact angles described by the Gibbs' inequality.

Conclusions

- Theoretical calculations assuming an ellipsoidal model for a rough particle gives the closest approximation of the maximum capillary force.
- Theoretical calculations assuming rounded shapes cannot provide estimates of snap-off forces experienced by particles due to pinning of air-water interfaces at sharp edges and corners of natural sediment particles.
- Pinning phenomena and snap-off forces can be calculated from the Gibbs extension of the Young-Laplace equation.
- Local pinning on particle surfaces due to roughness have a pronounced effect on the capillary forces and the local contact angles.

Implications

- Surface roughness and irregular shapes considerably increase capillary forces experienced by sediment particles, and such effects are even more important for colloids.
- Colloidal mobilization by air-water interfaces caused by water movement in soils are thus affected by particle shape and surface properties.
- Both mm-scale particles and colloids containing contaminants can be mobilized during infiltration and drainage.
- Enhanced mobilization of contaminants will be important to consider for the clean-up efforts at the Hanford Site.

Publications

- Nirmalya Chatterjee & Flury, M., Effect of particle shape on capillary forces on model particles and an air-water interface, *In preparation for submission to Langmuir*, **2013**
- Chatterjee, N., Lapin, S. & Flury, M., Capillary Forces between Sediment Particles and an Air–Water Interface, *Environmental Science & Technology*, **2012**, 46, 4411-4418.